NONLINEAR OPTICAL PHENOMENA

PACS numbers: 42.65.Ky; 42.79.Dj; 73.20.Mf
DOI: 10.1070/QE2007v037n03ABEH013220

Peculiarities of increasing the third harmonic generation efficiency upon noncollinear excitation of a surface plasmon on a metal diffraction grating

A.V. Andreev, A.A. Korneev, I.R. Prudnikov

***Abstract*. The efficiency of third harmonic generation (THG) upon noncollinear excitation of a surface plasmon on a metal diffraction grating is studied based on theoretical simulations. The basic channels of the nonlinear interaction of surface plasmons determining the intensity of the THG nonlinear response of the grating are considered. The influence of the period and groove depth of the diffraction grating on the THG efficiency is analysed.**

Keywords: *third optical harmonic, surface plasmon, diffraction grating.*

1. Introduction

Third harmonic generation (THG) is an efficient method for studying properties of thin metal films and nanoparticles on substrates [1]. Note in this connection THG experiments on measuring the thickness of metal films and the values of components of the third-order nonlinear susceptibility tensor [2, 3]. Spectra of the nonlinear response at the third harmonic frequency contain information on the shape and size of single nanoparticles [4] and their location on a surface [5].

The main problem of THG experiments is a low THG efficiency. For example, in the case of a gold film on a substrate, the ratio of the THG signal intensity $I(3\omega)$ to the pump radiation intensity $I(\omega)$ incident on a medium is $\sim 10^{-11}$ [6]. Aside from direct increasing the incident radiation intensity, the THG signal can be enhanced by increasing the nonlinear response of a metal by exciting surface plasmons [7]. A surface plasmon is a surface electromagnetic wave propagating along the metal – vacuum interface [8]. Surface plasmons are produced due to collective oscillations of conduction electrons in a metal. A surface plasmon is partially a longitudinal TM wave. The electric vector $\boldsymbol{E}$ in such a wave has one component directed along the plasmon wave vector and the other directed perpendicular to the metal surface [9].

A.V. Andreev, A.A. Korneev, I.R. Prudnikov Department of Physics, M.V. Lomonosov Moscow State University, Vorob'evy gory, 119992 Moscow, Russia; e-mail: korneev_anton@inbox.ru

Received 5 May 2006; revision received 8 August 2006
Kvantovaya Elektronika **37** (3) 259 – 265 (2007)
Translated by M.N. Sapozhnikov

Surface plasmons are excited due to energy transfer from the exciting bulk wave to a surface electromagnetic wave. Because a surface plasmon exists only in a thin surface layer (of thickness ~ 10 nm), the energy density of its electromagnetic field exceeds by several times the energy density of the pump wave. It is this circumstance that causes a great increase in the nonlinear response intensity and, hence, the THG enhancement in the case of efficient excitation of surface plasmons [10].

Note that the use of surface plasmons for increasing the THG efficiency is prevented by the fact that they cannot be directly excited by a bulk wave on a smooth metal surface. The dispersion relation for a surface plasmon

$$K_{\mathrm{SP}} = K\left(\frac{\varepsilon_1\varepsilon_2}{\varepsilon_1+\varepsilon_2}\right)^{1/2}, \qquad (1)$$

(where ε_1 and ε_2 are the dielectric susceptibilities of a metal and dielectric, respectively) shows that the modulus of its wave vector K_{SP} always exceeds the modulus $K = \omega/c$ of the wave vector of a bulk electromagnetic wave in vacuum [9]. At present several efficient methods are developed for compensating the difference of the wave vectors of a plasmon and exciting wave to obtain the phase matching condition: the prism method (the Otto [11] and Kretschmann [12] geometries) and the grating method (excitation by using a diffraction grating [13]). In the latter case, a metal film is deposited on a dielectric diffraction grating, and surface plasmons are excited by some of the diffraction orders of the exciting wave.

Surface plasmons can be excited on a diffraction grating collinearly or noncollinearly [14]. Upon collinear excitation, the grooves of the diffraction grating are perpendicular to the plane of incidence of the pump wave. The maximum excitation efficiency of surface plasmons in this geometry is achieved when the incident wave has the p polarisation. In the case of noncollinear excitation of surface plasmons, the grating grooves are parallel to the plane of incidence of light, and the incident wave has the s polarisation. A specific feature of the noncollinear scheme is the possibility to excite simultaneously two diffraction orders of the pump wave [14]. This considerably expands the spectrum of nonlinear interactions of various surface plasmons and also offers additional possibilities for controlling the excitation efficiency of surface plasmons and the spatial distribution of their electromagnetic field near the metal surface [15 – 18].

This paper is devoted to the analytic study and numerical simulation of the nonlinear response at the third harmonic frequency upon excitation of surface plasmons

during the diffraction of the pump wave from a metal diffraction grating.

2. Peculiarities of noncollinear excitation of surface plasmons

Consider in detail the THG process upon diffraction of laser radiation. Figure 1 presents the principal scheme of this process. The z axis of the Cartesian coordinate system used in Fig. 1 is perpendicular to a metal surface and is directed inside the metal, while the y axis is parallel to the reciprocal grating vector $\boldsymbol{Q}$ (where $Q = 2\pi/T$ and T is the grating period). The incident electromagnetic radiation with the wave vector $\boldsymbol{K}$ diffracts from the metal diffraction grating. The spatial spectrum of scattered radiation after diffraction contains the diffracted components of the field with the wave vectors

$$\boldsymbol{K}^{(m)} = \left\{K_x, K_y + mQ, \left[K^2 - K_x^2 - (K_y + mQ)^2\right]^{1/2}\right\}, \quad (2)$$

where $m = 0, \pm1, \pm2, \ldots$ is the diffraction order; K_x, K_y are the projections of the wave vector of incident radiation on the coordinate axes. The phase matching condition

$$\boldsymbol{K}_{\mathrm{t}}^{(m)} = \boldsymbol{K}_{\mathrm{t}} + m\boldsymbol{Q} = \boldsymbol{K}_{\mathrm{SP}} \quad (3)$$

required for efficient excitation of surface plasmons can be obtained by selecting properly the grating parameters. Here, $\boldsymbol{K}_{\mathrm{t}}^{(m)}$ and $\boldsymbol{K}_{\mathrm{t}}$ are the projections of the wave vectors of the mth diffraction order and incident radiation on the diffraction grating surface (plane xy), respectively. If the probability of diffraction to the mth order decreases with increasing $|m|$, the grating parameters are selected taking into account that condition (3) is fulfilled in the ±1st diffraction orders.

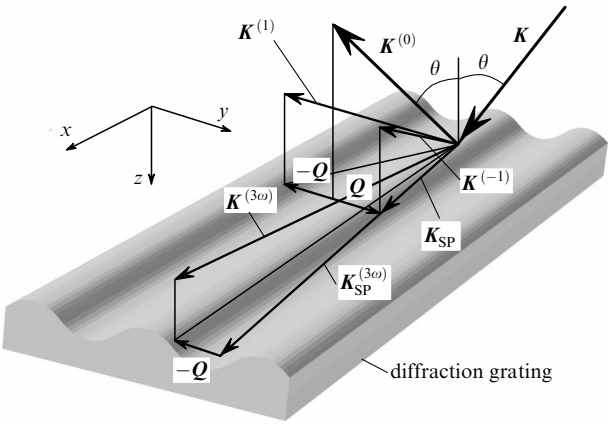

Figure 1. Principal scheme of the THG process upon excitation of surface plasmons on a diffraction grating: $\boldsymbol{Q}$ is the reciprocal grating vector; $\boldsymbol{K}$ is the wave vector of the incident wave; $\boldsymbol{K}^{(m)}$ is the wave vector of the mth diffraction order; $\boldsymbol{K}_{\mathrm{SP}}$ is the wave vector of the surface plasmon; $\boldsymbol{K}^{(3\omega)}$ is the wave vector of the THG bulk wave.

Due to excitation of surface plasmons at the pump frequency, the intensity of the electric field near the metal–vacuum interface increases, resulting in the enhancement of the nonlinear interaction between surface plasmons. The interaction between three plasmons leads to the appearance of a surface plasmon at the third harmonic frequency with the wave vector $\boldsymbol{K}_{\mathrm{SP}}^{(3\omega)} = 3\boldsymbol{K}_{\mathrm{SP}}$ (Fig. 1), whose modulus is greater than the modulus of the wave vector $K^{(3\omega)} = 3K$ of the bulk electromagnetic wave at the third harmonic frequency in vacuum. However, the moduli of the wave vectors of nonlinear waves obtained due to diffraction of surface plasmons at the third harmonic frequency from the grating can satisfy the inequality

$$K_{\mathrm{SP}}^{(3\omega)} > K^{(3\omega)} > \left|\boldsymbol{K}_{\mathrm{SP}}^{(3\omega)} + m\boldsymbol{Q}\right|. \quad (4)$$

Inequality (4) is the condition that the diffracted surface wave can be reemitted to the space over the diffraction grating. The efficiency of scattering to the mth diffraction order decreases with increasing $|m|$, and therefore a bulk wave produced due to single scattering of surface plasmons at the third harmonic frequency from the diffraction grating ($m = -1$) will have the greatest intensity.

Figure 2 shows the vector diagram illustrating the THG process upon noncollinear excitation of surface plasmons. As mentioned in Introduction, in the case of noncollinear excitation of surface plasmons, phase matching condition (3) is fulfilled simultaneously for two diffraction orders. Thus, two surface plasmons are excited simultaneously with the wave vectors $\boldsymbol{K}_{\mathrm{SP}} = \boldsymbol{K}_{\mathrm{t}} + \boldsymbol{Q}$ and $\boldsymbol{K}'_{\mathrm{SP}} = \boldsymbol{K}_{\mathrm{t}} - \boldsymbol{Q}$ in the 1st and -1st diffraction orders, respectively. The nonlinear interaction of surface plasmons with the same wave vectors results in excitation of two plasmons at the third harmonic frequency with the wave vectors $\boldsymbol{K}_{\mathrm{SP}}^{(3\omega)} = 3\boldsymbol{K}_{\mathrm{SP}}$ and $\boldsymbol{K}'^{(3\omega)}_{\mathrm{SP}} = 3\boldsymbol{K}'_{\mathrm{SP}}$. Scattering of surface plasmons at the third harmonic frequency from a metal diffraction grating gives rise to nonlinear waves with the wave vectors satisfying condition (4), which can be reemitted to the space:

$$\begin{aligned} &\left|\boldsymbol{K}_{\mathrm{SP}}^{(3\omega)} - \boldsymbol{Q}\right| < K^{(3\omega)}, \\ &\left|\boldsymbol{K}'^{(3\omega)}_{\mathrm{SP}} + \boldsymbol{Q}\right| < K^{(3\omega)}. \end{aligned} \quad (5)$$

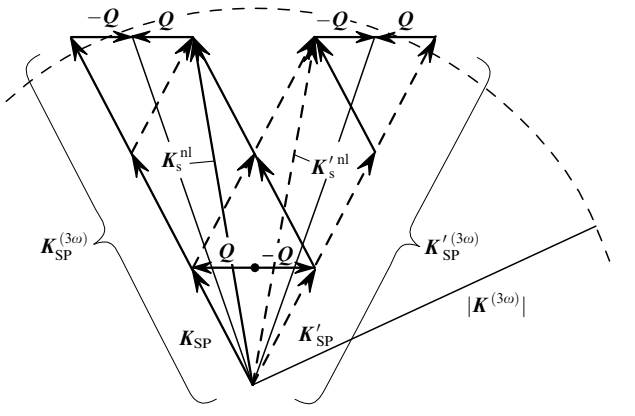

Figure 2. Vector diagram illustrating the THG process upon noncollinear excitation of surface plasmons on the diffraction grating: $\boldsymbol{Q}$ is the reciprocal grating vector; $\boldsymbol{K}$ is the wave vector of the incident wave; $\boldsymbol{K}_{\mathrm{SP}}$ and $\boldsymbol{K}'_{\mathrm{SP}}$ are the wave vectors of surface plasmons excited by the 1st and -1st diffraction orders of the pump wave, respectively; $\boldsymbol{K}_{\mathrm{SP}}^{(3\omega)}$ and $\boldsymbol{K}'^{(3\omega)}_{\mathrm{SP}}$ are the wave vectors of surface plasmons at the third-harmonic frequency; $\boldsymbol{K}_{\mathrm{s}}^{\mathrm{nl}}$ and $\boldsymbol{K}'^{\mathrm{nl}}_{\mathrm{s}}$ are the wave vectors of nonlinear waves at the third-harmonic frequency; $\boldsymbol{K}^{(3\omega)}$ is the wave vector of the bulk wave at the third-harmonic frequency; dashed curve is the arc of a circle of radius $|\boldsymbol{K}^{(3\omega)}|$ in the diffraction grating plane.

A specific feature of the noncollinearly excited THG process is the presence of the additional channel for reemission of the nonlinear surface wave to the space. This channel appears due to nonlinear interaction of surface plasmons with different spatial orientations of the wave vectors $\boldsymbol{K}_{\mathrm{SP}}$ and $\boldsymbol{K}'_{\mathrm{SP}}$. As a result, nonlinear waves are excited with the wave vectors satisfying the inequalities (Fig. 2)

$$K_{\mathrm{s}}^{\mathrm{nl}} = \left|\boldsymbol{K}_{\mathrm{SP}} + \boldsymbol{K}_{\mathrm{SP}} + \boldsymbol{K}'_{\mathrm{SP}}\right| < K^{(3\omega)}, \qquad K_{\mathrm{s}}'^{\mathrm{nl}} = \left|\boldsymbol{K}'_{\mathrm{SP}} + \boldsymbol{K}'_{\mathrm{SP}} + \boldsymbol{K}_{\mathrm{SP}}\right| < K^{(3\omega)}, \tag{6}$$

where $K_{\mathrm{s}}^{\mathrm{nl}}$ and $K_{\mathrm{s}}'^{\mathrm{nl}}$ are the moduli of the wave vectors of nonlinear surface waves. Thus, the simultaneous excitation of two surface plasmons makes possible the direct reemission of the nonlinear wave to space, without scattering from the diffraction grating. Note that upon single scattering of nonlinear waves with the wave vectors $\boldsymbol{K}_{\mathrm{s}}^{\mathrm{nl}}$ and $\boldsymbol{K}_{\mathrm{s}}'^{\mathrm{nl}}$ by the diffraction grating, the diffracted components appear with the wave vectors satisfying the conditions (Fig. 2)

$$\left|\boldsymbol{K}_{\mathrm{s}}^{\mathrm{nl}} + \boldsymbol{Q}\right| < K^{(3\omega)}, \quad \boldsymbol{K}_{\mathrm{s}}^{\mathrm{nl}} + \boldsymbol{Q} = \boldsymbol{K}_{\mathrm{SP}}^{(3\omega)} - \boldsymbol{Q}, \qquad \left|\boldsymbol{K}_{\mathrm{s}}'^{\mathrm{nl}} - \boldsymbol{Q}\right| < K^{(3\omega)}, \quad \boldsymbol{K}_{\mathrm{s}}'^{\mathrm{nl}} - \boldsymbol{Q} = \boldsymbol{K}_{\mathrm{SP}}'^{(3\omega)} + \boldsymbol{Q}. \tag{7}$$

Below, we will call the reemission channel for the waves described by expression (6) the interaction channel and the channel related to expressions (5) and (7) – the diffraction channel. The intensities of signals at the third harmonic frequency for these channels can be detected separately in experiments because their spatial orientation coincides with that of the wave vectors of different diffraction orders at the third harmonic frequency:

$$\boldsymbol{K}_{\mathrm{s}}^{\mathrm{nl}} + \boldsymbol{Q} = \boldsymbol{K}_{\mathrm{SP}}^{(3\omega)} - \boldsymbol{Q} = \boldsymbol{K}_{\mathrm{t}}^{(3\omega)(2)}, \quad \boldsymbol{K}_{\mathrm{s}}^{\mathrm{nl}} = \boldsymbol{K}_{\mathrm{t}}^{(3\omega)(1)}, \qquad \boldsymbol{K}_{\mathrm{s}}'^{\mathrm{nl}} + \boldsymbol{Q} = \boldsymbol{K}_{\mathrm{SP}}'^{(3\omega)} - \boldsymbol{Q} = \boldsymbol{K}_{\mathrm{t}}^{(3\omega)(-2)}, \quad \boldsymbol{K}_{\mathrm{s}}'^{\mathrm{nl}} = \boldsymbol{K}_{\mathrm{t}}^{(3\omega)(-1)}, \tag{8}$$

where $K_{\mathrm{t}}^{(3\omega)(m)} = \left[(3K\sin\theta)^2 + (mQ)^2\right]^{1/2}$ is the projection of the wave vector of the mth diffraction order on the underlying surface at the third harmonic frequency. Thus, by analysing the intensity of the THG signals in the directions of the $\pm$1st and $\pm$2nd diffraction orders, we can study the efficiency of the diffraction and interaction channels, respectively, and estimate the total THG efficiency, which is proportional to the sum of the THG intensities from all diffraction orders for a fixed angle of incidence of the pump beam.

3. Theoretical model and calculation method

We simulated the THG process upon diffraction of electromagnetic radiation from a metal diffraction grating by the method of recurrent relations [19]. This method is based on the division of the initial profile of the surface relief into N inhomogeneous layers of thickness d separated by infinitely thin vacuum gaps. The parameter d is selected based on the following assumptions:

(i) The change in the electric-field amplitude of the incident wave propagated through a layer is negligible small;

(ii) reflection of light from the layer is negligible compared to its transmission through the layer.

Taking these assumptions into account, the reflection and transmission coefficients of the layer can be calculated analytically by using the vector Maxwell equations [19]. Due to periodic variations in the optical parameters of the medium along the layer, the incident field $\boldsymbol{E}^{\mathrm{t}}(\boldsymbol{r}, t)$ can be represented as a superposition of Bloch waves:

$$\boldsymbol{E}^{\mathrm{t}}(\boldsymbol{r}, t) = \sum_n \boldsymbol{E}_n^{\mathrm{t}} \exp(\mathrm{i}K_x x + \mathrm{i}K_y y + \mathrm{i}Qny + \mathrm{i}K_z^{(n)} z - \mathrm{i}\omega t), \tag{9}$$

where $\boldsymbol{E}_n^{\mathrm{t}}$ are the amplitudes of Bloch waves; K_x and K_y are the projections of the wave vector of incident radiation on the coordinate axes; and $K_z^{(n)} = [K^2 - K_x^2 - (K_y + nQ)^2]^{1/2}$. A similar expression can be written for the field $\boldsymbol{E}^{\mathrm{s}}(\boldsymbol{r}, t)$ reflected from the layer. Then, recurrent relations are written which relate the field incident on the jth layer (subscript t) with the field scattered by this layer (subscript s):

$$\hat{E}_j^{\mathrm{t}} = \hat{\tau}_{j-1}\hat{E}_{j-1}^{\mathrm{t}} + \hat{s}'_{j-1}\hat{E}_j^{\mathrm{s}}, \qquad \hat{E}_j^{\mathrm{s}} = \hat{s}_j\hat{E}_j^{\mathrm{t}} + \hat{\tau}'_j\hat{E}_{j+1}^{\mathrm{s}}, \tag{10}$$

where $\hat{E}_j^{\mathrm{t}}$ and $\hat{E}_j^{\mathrm{s}}$ are column matrices of the amplitudes of Bloch waves, which determine the field incident on the jth layer and reflected from it, respectively; $\hat{s}_j$ and $\hat{\tau}_j$ are matrices for the reflection and transmission of the layer, respectively; and $\hat{s}'_j$ and $\hat{\tau}'_j$ describe the reflection and transmission of the waves incident on the opposite side of the jth layer. Recurrent relations (10) are used for vacuum gaps, beginning from the gap over a substrate, for which the incident and reflected fields are related by the Fresnel coefficients: $\hat{E}_0^{\mathrm{s}} = \hat{R}_{\mathrm{sub}}\hat{E}_0^{\mathrm{t}}$, where the matrix $\hat{R}_{\mathrm{sub}}$ contains Fresnel coefficients for reflection from a plane semi-infinite substrate. The step-by-step application of system (10) for all vacuum gaps allows us to find the reflection coefficient of the relief as a whole and the electric field strength $\boldsymbol{E}_j$ at the pump frequency inside each layer. Then, nonlinear polarisation is calculated at the third harmonic frequency inside each layer in the fixed-pump-field approximation:

$$P_{ij}^{\mathrm{nl}(3\omega)} = \hat{\chi}_{inkl}^{(3)} E_{nj} E_{kj} E_{lj}, \tag{11}$$

where $P_{ij}^{\mathrm{nl}(3\omega)}$ is the Cartesian component on nonlinear polarisation at the third harmonic frequency inside the jth layer; $\hat{\chi}_{inkl}^{(3)}$ is the tensor of nonlinear cubic susceptibility; and $i, n, k, l = x, y, z$. We calculated nonlinear polarisation by using the model of a homogeneous and isotropic medium. In this case, the tensor $\hat{\chi}_{inkl}^{(3)}$ has 21 nonzero components, the three components being linearly independent. By knowing nonlinear polarisation, we can calculate the nonlinear response of a layer. The nonlinear response of the entire grating is found by writing recurrent relations, which are similar to Eqns (10), but for the fields at the third harmonic frequency inside the vacuum gap over the jth layer. In this case, the presence of sources of

nonlinear response inside the layer is taken into account [see expression (11)]:

$$\hat{E}_j^{\mathrm{t}} = \hat{\tau}_{j-1}\hat{E}_{j-1}^{\mathrm{t}} + \hat{s}'_{j-1}\hat{E}_j^{\mathrm{s}} + \hat{E}_{j-1}^{\mathrm{t\,nl}},$$
$$\hat{E}_j^{\mathrm{t}} = \hat{s}_j\hat{E}_j^{\mathrm{t}} + \hat{\tau}'_j\hat{E}_{j+1}^{\mathrm{s}} + \hat{E}_j^{\mathrm{s\,nl}}, \qquad (12)$$

where $\hat{E}_j^{\mathrm{s\,nl}}$ и $\hat{E}_j^{\mathrm{t\,nl}}$ are column matrices containing the nonlinear Bloch components of the field at the third harmonic frequency, which are emitted by the jth layer to vacuum gaps over and under the layer, respectively. The filed intensity at the third harmonic frequency incident from vacuum on the grating is zero ($\hat{E}_N^{\mathrm{t}} = 0$). The incident and reflected fields in the vacuum gap over the substrate are related by Fresnel coefficients. By taking these boundary conditions into account, we can find the matrix $\hat{E}_N^{\mathrm{s}}$ containing the amplitudes of the waves for different third-harmonic diffraction orders which are diffracted from the grating to vacuum. The algorithm described above allows one to find the intensity and polarisation components of the third harmonic for any diffraction order and any spatial orientation of the wave vector of pump radiation incident on the diffraction grating.

4. Increasing the THG efficiency due to excitation of surface plasmons

Figure 3 presents the intensities of the third harmonic reemitted in the directions of different diffraction orders as functions of the angle of incidence of pump radiation for a thin gold film deposited on a glass substrate with the sinusoidal relief $z = H\,[1 + \sin(Qy)]$, where H is the relief height. The calculation was performed by using the algorithm described in section 3. The film thickness was 35 nm, the relief height was 100 nm, the wavelength of the incident s-polarised radiation was 810 nm, and the grating period was 1140 nm. (A sample with these parameters was used in the experimental THG study [20].) The excitation of surface plasmons leads to the appearance of the minimum [13] of the curve of specular reflection of light from the diffraction grating (see the solid curve in Fig. 3). One can see that the excitation of surface plasmons causes a considerable enhancement of the third harmonic for all diffraction orders (the maxima of the third-harmonic signals correspond to the minimum of the reflection coefficient), which demonstrates the increase in the THG efficiency. In this case, third-harmonic signals propagating in vacuum in the direction of the $\pm$1st and $\pm$2nd diffraction orders have the same intensity. This follows directly from the general symmetry of the problem of noncollinear propagation of light on a diffraction grating with respect to the diffraction-grating relief profile (see Fig. 2). As mentioned in section 2, the third-harmonic wave propagating in the direction of the 1st (and $-$1st) diffraction order is reemitted to vacuum via the diffraction channel, whereas in the case of the 2nd (and $-$2nd) diffraction order, the interaction channel is involved. Below, we will study the efficiency of these channels by using the first and second third-harmonic diffraction orders.

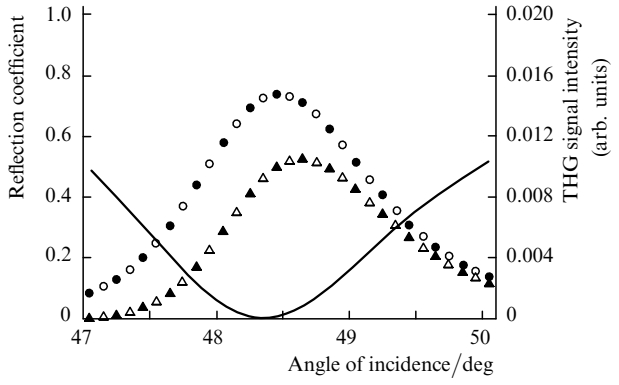

Figure 3. Dependences of the THG signal intensities reemitted in the 1st (▲), $-$1st (△), 2nd (●), and $-$2nd (○) diffraction orders and of the reflection coefficient of the diffraction grating (solid curve) on the angle of incidence of the pump wave upon excitation of surface plasmons ($T = 1140$ nm).

5. Influence of the diffraction grating period on the THG efficiency

Figure 4 presents the intensities of the third harmonic as function of the angle of incidence of pump radiation for the grating period $T = 815$ nm (the rest of the grating and incident radiation parameters are as in Fig. 3). A comparison of the curves in Figs 3 and 4 shows that for a greater grating period ($T = 1140$ nm, Fig. 3), the third-harmonic signal for the second diffraction order is more intense than that for the first diffraction order, whereas in the case of a smaller grating period ($T = 815$ nm, Fig. 4), the third-harmonic signal for the first diffraction order is stronger. (This change in the signal intensities will be explained in section 6.) The main difference between Figs 3 and 4 is that the third-harmonic signal for both reemission channels increased by an order of magnitude with decreasing the grating period.

To explain this difference in the THG signals, we study the dependence of the excitation efficiency of surface plasmons on the diffraction grating period. Numerical simulations showed that the excitation of surface plasmons leads to the resonance enhancement of the intensities of the 1st and $-$1st diffraction orders at the pump wave frequency on the grating surface for $z = 0$. Simulations were performed by using the algorithm described in section 3, which also allows us to calculate the intensities of the s- and p-

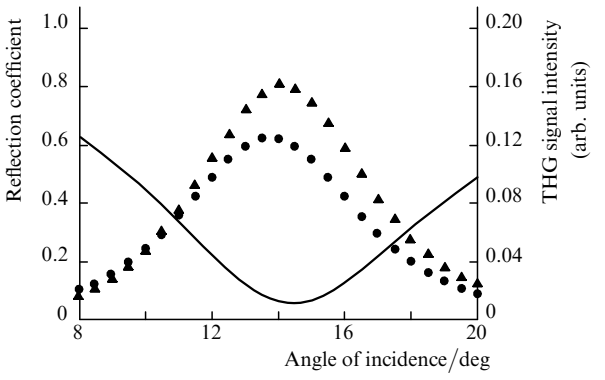

Figure 4. Dependences of the THG signal intensities reemitted in the first (▲) and second (●) diffraction orders and of the reflection coefficient of the diffraction grating (solid curve) on the angle of incidence of the pump wave upon excitation of surface plasmons ($T = 815$ nm).

polarised components of the mth diffraction order, respectively,

$$I_s^{(m)} = \left[E_y^{(m)} \frac{\boldsymbol{K}_t \boldsymbol{K}_t^{(m)}}{|\boldsymbol{K}_t||\boldsymbol{K}_t^{(m)}|}\right]^2 + \left[E_x^{(m)} \frac{m\boldsymbol{Q}\boldsymbol{K}_t^{(m)}}{|m\boldsymbol{Q}||\boldsymbol{K}_t^{(m)}|}\right]^2,$$
$$I_p^{(m)} = E_x^{(m)2} + E_y^{(m)2} + E_z^{(m)2} - I_s^{(m)}, \quad (13)$$

where $E_x^{(m)}$, $E_y^{(m)}$, and $E_z^{(m)}$ are the projections of the field strength vector in the mth diffraction order on the axes of the Cartesian coordinate system for $z = 0$. Because of the symmetry of the problem, the intensities of the $m = \pm 1$ diffraction orders are the same, and therefore we will present below the results obtained for $m = 1$.

Figure 5a shows the dependences of the specular reflection coefficient of a diffraction grating and the field intensity in the first diffraction order (FDO) at the pump frequency on the angle of incidence of pump radiation. The field intensity was calculated for $z = 0$. In addition, the intensities of the s- and p-polarised components of the FDO field are presented. Calculations were performed for the grating period $T = 1140$ nm. One can see that at the point of excitation of surface plasmons (in the vicinity of the minimum of the specular reflection coefficient), the FDO intensity has a maximum caused by the resonance amplification of its p-polarised component. The latter circumstance is a direct consequence of the type of polarisation of surface plasmons. The electric field vector of surface plasmons lies in the plane formed by its wave vector [which in the case of phase matching condition (3) coincides with the projection of the FDO wave vector on the underlying surface] and the normal to the underlying surface. The s-polarised component of the FDO electric field is perpendicular to this surface and cannot be involved in the excitation of surface plasmons. Thus, surface plasmons are excited by the p-polarised FDO component, and the increase in its intensity indicates excitation of surface waves.

Consider now the dependences of the FDO intensity and polarisation on the diffraction grating period. Figure 5b presents the dependences of the FDO intensity and its polarisation components at the point of excitation of surface plasmons on the grating period. One can see that the FDO intensity increases with decreasing the grating period, which means that the excitation efficiency of surface waves increases. The fraction of the p-polarised component of the FDO field also increases. Thus, the intensity ratio $I_p^{(1)}/I_s^{(1)}$ of the p- and s-polarised components of the FDO electric field for grating periods $T = 1140$ and 815 nm was 4 and 8.5, respectively.

Let us present the physical explanation of the increase in the p-polarised component with decreasing the diffraction grating period. Figure 6 shows the vector diagram illustrating the spatial position of the projections of the wave vectors of incident radiation and FDO on the underlying surface and the orientation of the electric field vector of the incident wave for two grating periods. The angle of incidence was selected based on the phase matching condition (3). As the grating period decreases, the angle ψ between the electric field vector of incident radiation and the FDO wave vector (Fig. 6) also decreases. This results in the increase in the projection $E' = E\cos\psi$ of the electric field vector $\boldsymbol{E}$ of the incident wave on the projection $\boldsymbol{K}_t^{(1)}$ of the FDO wave vector. As a result, the p-polarised component of the electric FDO field will increase, while the s-polarised component will decrease. Because surface polaritons are excited by the p-polarised component of the FDO field, the decrease in the grating period leads to the increase in the excitation efficiency of surface polaritons. As a result, the local field of surface polaritons increases (the average normalised electric field strengths $\langle E_{met}\rangle$ calculated at the pump frequency in a metal film for $T = 1140$ and 815 nm are 14 and 32, respectively), and hence nonlinear polarisation at the THG frequency also increases [see (11)]. This leads to

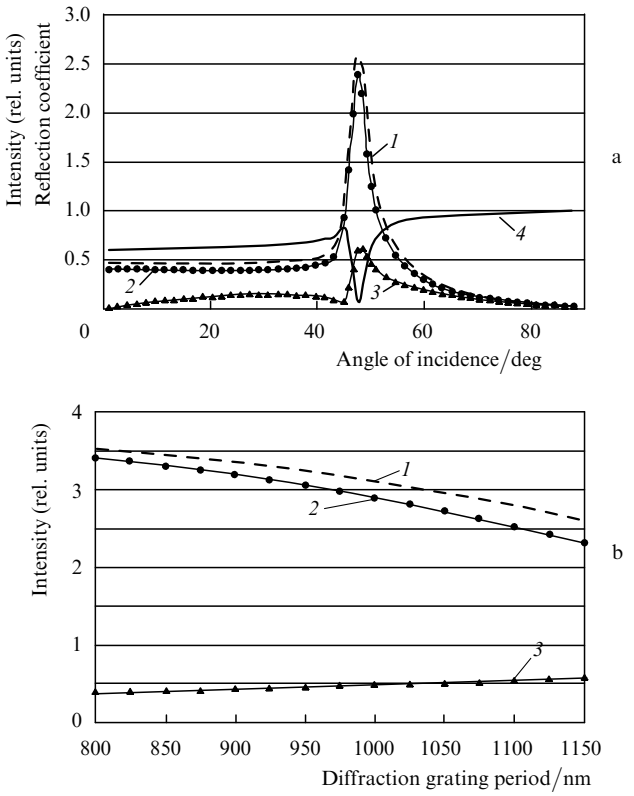

Figure 5. Dependences of the FDO intensity at the pump frequency (*1*), intensities of the p-polarised (*2*) and s-polarised (*3*) components of the FDO field and of the reflection coefficient of the diffraction grating (*4*) on the angle of incidence ($T = 1140$ nm) (a) and the diffraction grating period (the angle of incidence of the pump wave corresponds to the point of excitation of surface plasmons) (b).

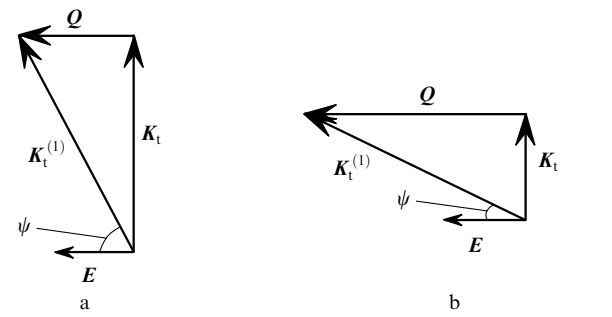

Figure 6. Vector diagrams of scattering of the pump radiation to the first diffraction order for grating periods $T = 1140$ (a) and 815 nm (b) upon excitation of surface plasmons: $\boldsymbol{Q}$ is the reciprocal grating vector; $\boldsymbol{K}_t$, $\boldsymbol{K}_t^{(1)}$ are the projections of the wave vectors of the incident wave and FDO on the underlying surface; $\boldsymbol{E}$ is the electric field strength vector of the incident wave.

the increase in the third-harmonic signal in all diffraction orders.

6. Influence of the diffraction-grating relief height of the THG efficiency

Let us study now the influence of the diffraction-grating relief on the THG efficiency. Consider the excitation dynamics of surface polaritons with increasing the grating relief height. Figure 7 shows the calculated dependences of the FDO field intensity and the polarisation components of this field on the relief height at the excitation point of surface polaritons. One can see that the FDO intensity curve has a maximum at the relief height $H = 160$ nm; then it decreases and for $H \approx 200$ nm acquires its initial value at $H = 100$ nm. Thus, surface plasmons are excited most efficiently (and hence the enhancement of the local field is maximal) at $H = 160$ nm. As the relief height is further increased, the excitation efficiency of surface plasmons decreases.

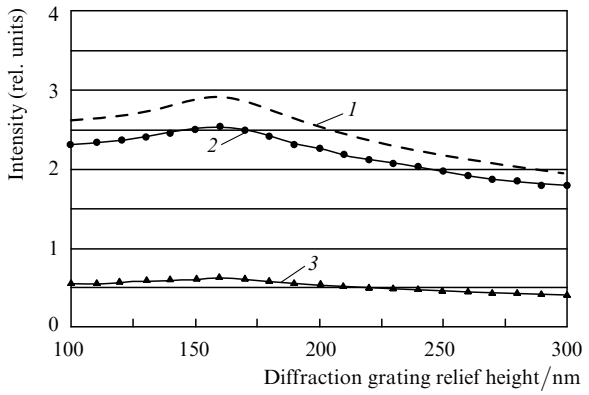

Figure 7. Dependences of the FDO intensity at the pump frequency (*1*) and the intensities of the p-polarised (*2*) and s-polarised (*3*) components of the FDO field on the diffraction grating relief height.

A change in the excitation efficiency of surface plasmons with increasing the relief height is caused by the increase in the efficiency of scattering from the diffraction grating. In the case of small relief heights ($H < 160$ nm), this results in the enhancement of excitation of surface plasmons [21] [single scattering of the pump wave by the diffraction grating, see (3)], while for high enough relief heights ($H > 160$ nm), this leads to the interaction of two excited surface plasmons [16] (double scattering of surface plasmons by the diffraction grating):

$$\boldsymbol{K}_{\mathrm{SP}} - \boldsymbol{Q} - \boldsymbol{Q} = \boldsymbol{K}'_{\mathrm{SP}}, \qquad \boldsymbol{K}'_{\mathrm{SP}} + \boldsymbol{Q} + \boldsymbol{Q} = K_{\mathrm{SP}}. \tag{14}$$

This interaction of surface plasmons results in the decrease in the excitation efficiency of both plasmons [16] for relief heights $H > 160$ nm. Note that, unlike the dependence presented in Fig. 5b, the FDO field intensity increases almost without a change in the intensity ratio of the polarisation components of the field $[I_{\mathrm{p}}^{(1)}/I_{\mathrm{s}}^{(1)} = 4$ for $H = 100$ nm and 4.3 for $H = 160$ nm]. This is explained by the fact that, as the grating relief height increases, the spatial positions of the electric field vector of incident radiation and the FDO wave vector remain invariable. Therefore, according to the mechanism of a change in the FDO field polarisation described in section 5, the intensity ratio of the polarised FDO components will be also invariable.

The third-harmonic signal intensities calculated for different grating-relief heights for two diffraction orders as functions of the angle of incidence of pump radiation completely confirm our conclusions (Fig. 8). The maximum intensity of the third-harmonic signal is observed for both diffraction orders for the relief height $H = 160$ nm corresponding to the maximum excitation efficiency of surface plasmons. One can see that, as the grating-relief height increases, the third-harmonic signal intensity in the first diffraction order becomes greater than that in the second diffraction order. This effect can be explained by taking into

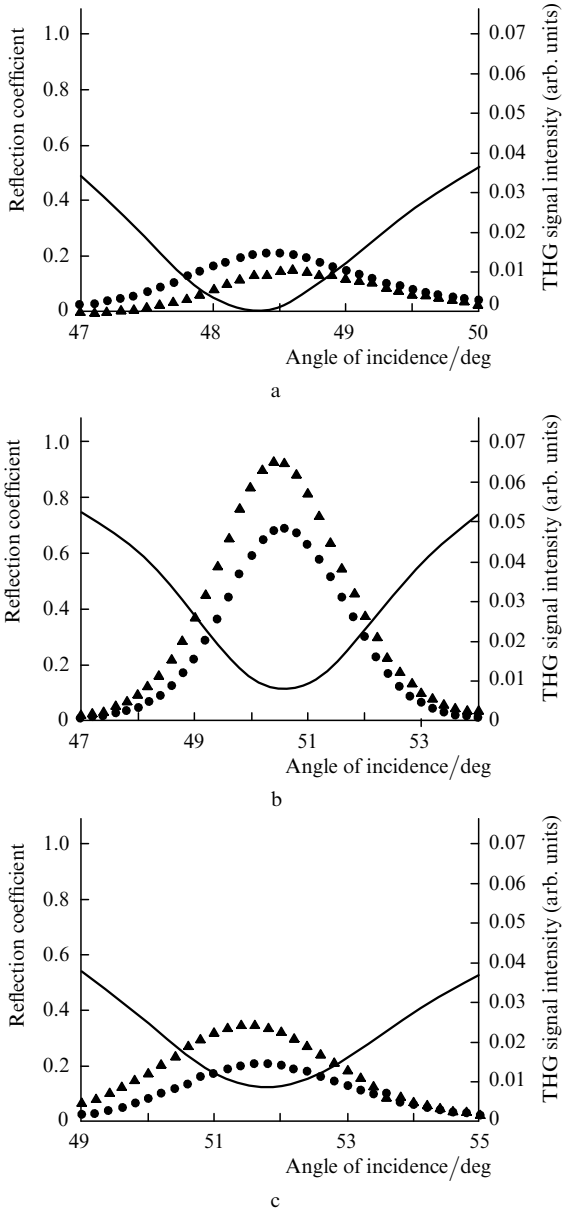

Figure 8. Dependences of the THG intensities reemitted in the first (▲) and second (●) diffraction orders and of the reflection coefficient of the diffraction grating (slid curve) on the angle of incidence of the pump wave upon excitation of surface plasmons for the relief heights $H = 100$ (a), 160 (b), and 240 nm (c).

account reemission channels for each of the third-harmonic diffraction orders (see section 4). In the case of small relief heights, reemission via the interaction channel (6) has a higher probability because, unlike the diffraction channel (5), (7), scattering from the diffraction grating is absent in this channel. The increase in the grating-relief height results in the increase in the single scattering efficiency, which in turn enhances the probability of processes (5), (7) and therefore the efficiency of the diffraction channel. Therefore, in the case of large relief heights, the probability of reemission via the diffraction channel will be higher than that via the interaction channel. The above analysis of the change in the relative intensity of third-harmonic diffraction orders suggests that the increase in the first-order third-harmonic diffraction intensity compared to the second-order diffraction intensity with decreasing the relief period (see Figs 3 and 4) is also explained by the increase in the scattering efficiency by the diffraction grating.

7. Conclusions

We have studied theoretically the THG efficiency upon noncollinear excitation of surface plasmons in a metal diffraction grating. The study was performed by using the numerical algorithm that we developed for calculating the nonlinear response of the diffraction grating. It has been shown that the excitation of surface plasmons results in the twenty-fold increase in the THG intensity. It has been found that upon noncollinear excitation of surface plasmons, there exist two channels of reemission of the THG surface waves to space. The intensity of the THG signals detected in different diffraction orders are determined by the efficiencies of these channels. In this case, the mirror symmetry of the intensities of the THG diffraction orders with respect to the zero order is a direct consequence of the symmetry of the problem of noncollinear scattering of light by the diffraction grating.

We have also investigated the THG efficiency as functions of the diffraction grating period and relief height. It has been shown that the dependence of THG intensity on these parameters is determined by the excitation efficiency of surface plasmons. The excitation efficiency of surface plasmons increases with decreasing the diffraction grating period. This is explained by the increase in the projection of the electric-field vector of the pump wave on the polarisation plane of surface plasmons. The THG intensity at different diffraction grating-relief heights depends on processes of scattering from the diffraction grating and has a maximum corresponding to the maximum excitation of surface plasmons.

Acknowledgements. This work was partially supported by the Russian Foundation for Basic Research (Grant No. 05-02-16764).

References

1. Barille R., Canioni L., Sarger L. *Phys. Rev. E*, **66**, 067602 (2002).
2. Schins M., Schrama T. *Opt. Soc. Am. B*, **19**, 1627 (2002).
3. Zhang C., Wu. X., Wu S. *Phys. Rev. B*, **54**, 16349 (1996).
4. Mikhailovsky A.A., Petruska M.A., Stockman M. *Phys. Rev. B*, **69**, 085401 (2004).
5. Yelin D., Oron D., Thiberge S. *Opt. Express*, **11**, 1385 (2003).
6. Farkas G., Toth Cs. *Phys. Rev. A*, **46**, R3605 (1992).
7. Tsang T. *Opt. Lett.*, **21** (4), 245 (1996).
8. Shen Y.R. *The Principles of Nonlinear Optics* (New York: Wiley, 1984; Moscow: Nauka, 1989).
9. Libenson M.N. *Soros Obraz. Zh.*, (10), 92 (1996).
10. Akhmanov S.A., Seminogov V.N., Sokolov V.I. *Zh. Eksp. Teor. Fiz.*, **93**, 1654 (1987).
11. Otto A. *Zr. Phys.*, **216**, 398 (1968).
12. Kretschmann E. *Zr. Phys.*, **241**, 313 (1971).
13. Teng Y., Stern E. *Phys. Rev. Lett.*, **19**, 511 (1967).
14. Agranovich V.M., Mills D.L. (Eds) *Surface Polaritons* (Amsterdam: North-Holland, 1982; Moscow: Nauka, 1985).
15. Kreiter M., Mittler S., Sambles J.R. *Phys. Rev. B*, **65**, 125415 (2002).
16. Fischer B., Fischer T., Knoll W. *Appl. Opt.*, **34**, 5773 (1995).
17. Andreev A.V., Korneev A.A., Mukina L.S., Nazarov M.M., Prudnikov I.R., Shkurinov A.P. *Kvantovaya Elektron.*, **35**, 27 (2005) [*Quantum Electron.*, **35**, 27 (2005)].
18. Kondratenko P.S. *Kvantovaya Elektron.*, **13**, 2009 (1986) [*Sov. J. Quantum Electron.*, **16**, 1326 (1986)].
19. Andreev A.V., Nazarov M.M., Prudnikov I.R., Shkurinov A.P., Masselin P. *Phys. Rev. B*, **69**, 035403 (2003).
20. Andreev A.V., Korneev A.A., Nazarov M.M., Prudnikov I.P., Shkurinov A.P. *Trudy tret'ei mezhdunarodnoi konferentsii 'Fundamental'nye problemy optiki'* (Proceeding of the 3rd International Conference of the Fundamental Problems of Optics) (St. Petersburg, St. Petersburg State University, 2004) p. 242.
21. Barnes W.L., Preist T.W., Kiston S.C., Sambles J.R. *Phys. Rev. B*, **54**, 6627 (1996).